*Bangladesh Journal of Physics, Vol. **32**, Issue 2, pp. 29 – 41, December 2025*

DESIGN AND DEFORMATION ANALYSIS OF MEMS PIEZORESISTIVE PRESSURE SENSORS USING COMSOL FOR SENSITIVITY ENHANCEMENT VIA MATERIAL OPTIMIZATION

MUKTADIR RAHMAN[1], SHOVON SAHA[1], SHAHRIAR EMON[1], MD. ASADUZZAMAN[1], KEYA ALOM[2] AND MD. KHORSHED ALAM[1,*]

[1]*Department of Physics, University of Barishal, Barishal-8254, Bangladesh*
[2]*Department of Electrical Electronic and Communication Engineering, Pabna University of Science & Technology, Pabna-6600, Bangladesh*

[*]*Corresponding author email: dmkalam@bu.ac.bd*
Received on 22.08.2025, Revised received on 10.11.2025, Accepted for publication on 04.12.2025

DOI: *https://doi.org/10.3329/bjphy.v32i2.83863*

ABSTRACT

Piezoresistive pressure sensors are critical in aerospace, biomedical and industrial applications where high sensitivity and reliability are essential. This study presents a simulation-based performance analysis of MEMS piezoresistive pressure sensors using COMSOL Multiphysics 6.1. Four materials—Aluminum Gallium Arsenide (AlGaAs), Germanium (Ge), Silicon (Si) and Titanium Germanium Carbide (Ti_3GeC_2)—were evaluated under identical sensor architectures. The design features a square diaphragm with an X-shaped piezoresistor layout to intensify stress concentration and boost sensitivity. Simulations were conducted under pressure load of 100 kPa. Key performance indicators—diaphragm displacement, shear and von Mises stress and sensitivity (V/Pa)—were analyzed. Ti_3GeC_2 exhibited the highest sensitivity (5.08×10^{-6} V/Pa), outperforming Si by 49% and showed superior mechanical resilience with the lowest deflection. These results highlight Ti_3GeC_2 as a promising candidate for next-generation MEMS sensors operating in harsh environments. The model is built on fabrication-relevant parameters and provides predictive insight into material selection for high-performance piezoresistive sensors.

Keywords: *MEMS pressure sensor, Piezoresistive effect, COMSOL Multiphysics, Ti_3GeC_2, Sensitivity analysis, Diaphragm deformation*

1. INTRODUCTION

Piezoresistive pressure sensors play a fundamental role in precision measurement systems across various industries, including aerospace, biomedical devices, industrial automation and automotive applications [1]. These sensors operate based on the piezoresistive effect, where mechanical stress alters the electrical resistance of a sensing element, which is then measured using a Wheatstone bridge circuit [2]. The ability to achieve high sensitivity, fast response time and miniaturization has made Microelectromechanical Systems (MEMS)-based piezoresistive pressure sensors a widely adopted choice in modern sensing technology[3]. However, conventional silicon-based piezoresistive sensors exhibit limitations, particularly in high-temperature and harsh environmental conditions, necessitating the exploration of alternative sensing materials with superior mechanical strength, thermal stability and electrical performance [4,5].

Many researchers have worked on optimizing the geometry and design of MEMS piezoresistive pressure sensors such as [6,7].

However, not much attention has been given to how different piezoresistive materials behave under the same conditions. Most previous research focused primarily on silicon-based designs, overlooking alternative materials that could provide higher sensitivity and greater thermal stability [6-8]. Therefore, the motivataion of this work is to perform a comprehensive simulation-based comparison of four materials-AlGaAs, Ge, Si, and Ti_3GeC_2 to identify the most efficient and reliable material for high-performance MEMS pressure sensors operating in harsh environments.

The sensitivity and performance of a piezoresistive pressure sensor depend on several key factors, including the diaphragm's mechanical properties, stress distribution, piezoresistor placement and the intrinsic characteristics of the sensing material [8,9]. Traditionally, silicon (Si) has been the dominant material due to its mature fabrication process, compatibility with semiconductor technology and well-characterized piezoresistive properties [10]. However, Si-based sensors suffer from increased leakage current, a low bandgap (1.12 eV) and thermal instability, limiting their application in extreme environments such as high-temperature aerospace propulsion systems or industrial process monitoring [11]. To overcome such limitations, mechanically stable and large-bandgap compounds such as titanium germanium carbide (Ti_3GeC_2), germanium (Ge) and aluminum gallium arsenide (AlGaAs) have been proposed as viable replacements [12,13].

In our study, we chose four materials—Si, Ge, AlGaAs, and Ti_3GeC_2—because each materials brings unique properties. Silicon is included as the conventional material and serves as a baseline for comparison. Germanium and AlGaAs were selected for their higher carrier mobility and tunable bandgap, which can improve sensitivity under certain conditions. Ti_3GeC_2, a MAX-phase material, was added due to its remarkable thermal and mechanical stability, making it suitable for harsh environments. By comparing these materials under identical structural conditions, we can clearly see how the inherent properties of each material affect sensor performance.

MAX-phase materials such as Ti_3GeC_2 has gained significant attention due to its high Young's modulus (~353 GPa), excellent thermal stability (operating beyond, chemical inertness and low thermal expansion coefficient, making it well-suited for applications in extreme environments [14]. MAX-phase materials such as Ti_3GeC_2 offer an optimal combination of metallic and ceramic properties, with high electrical conductivity, superior oxidation resistance and high-temperature stability, positioning them as competitive candidates for next-generation pressure sensors [15]. Additionally, Ge and AlGaAs have demonstrated potential due to their higher carrier mobility and tunable bandgap, which can enhance sensor signal-to-noise ratio and sensitivity under specific operating conditions [16,17]. A comparative study of these materials under the same conditions must be done to decide the most desirable piezoresistive sensing material and diaphragm configuration for high-performance MEMS pressure sensors.

Recent advancements in simulation computation software have enabled precise modeling of sensor behavior, piezoresistive and stress distribution response under varied conditions. COMSOL Multiphysics, a finite element analysis program, has widely been employed in modeling MEMS-based sensors and has allowed material deformation, electrical response and structural integrity to be explored in detail [18]. Optimization of piezoresistor position, diaphragm thickness and piezoresistive material selection can be achieved by Multiphysics simulation to achieve maximum sensitivity and reliability [19].

In this, a systematic simulation-based investigation of MEMS piezoresistive pressure sensors is discussed with focus on material choice and structural design optimization for increased sensitivity. Mechanical deformation, stress concentration and electrical output of AlGaAs, Ge, Si and Ti_3GeC_2

are investigated using COMSOL Multiphysics 6.1 under identical operating conditions. Sensor structure consists of a square diaphragm and X-shaped piezoresistor geometry, which are positioned at strategic high-stress locations to maximize output.

The X-configuration was utilized due to its capability of orienting piezoresistive elements along the principal stress directions, especially at the corners of the diaphragm where the maximum stress concentration is located. Previous research has indicated that these kinds of configurations have much better piezoresistive performance than traditional linear configurations through maximum strain-induced resistance changes [8,9]. By applying this same geometry to all materials, we can ensure that performance differences arise solely from inherent material behavior and not from structural variation. The results provide important information for the development of the next generation of piezoresistive pressure sensors, namely for applications requiring stable performance in severe environments where conventional Si-based sensors are unsuitable.

2. METHODOLOGY AND WORKING PRINCIPLE

The piezoresistive pressure sensor works by converting applied pressure into an electrical signal. When pressure is applied to the diaphragm, it bends slightly, creating mechanical stress in the piezoresistors. This stress changes their electrical resistance. A Wheatstone bridge circuit measures these resistance changes, producing a voltage output proportional to the applied pressure.

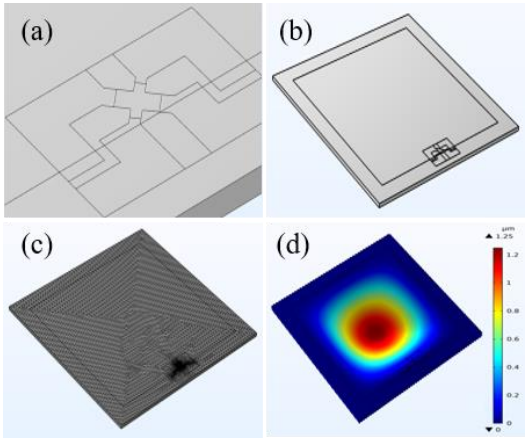

Fig. 1. (a) X-geometry of piezoresistors, (b) Constant area of lower surface diaphragm, (c) Mesh of the proposed model and (d) Deformation of pressure sensor diaphragm at 100 kPa. Mesh refinement was used in high stress areas for the assurance of structural and electrical accuracy.

The diaphragm is a square membrane (1 mm × 1 mm) with a thickness of 20 μm. Piezoresistors are arranged in an X-shaped pattern at the diaphragm corners (Fig. 1), where stress is highest, to maximize sensitivity. Fixed regions prevent unwanted movement, while the free areas deform under pressure, enabling accurate stress-to-resistance conversion.Using COMSOL Multiphysics, the upper and lower surfaces of the membrane were defined. The bottom membrane area was subtracted from the top surface and fixed to simulate the boundary conditions. The free region deforms under applied force, while the fixed areas remain stationary (Fig.1b). Proper electrical connections around the piezoresistors are critical for accurate sensor performance.

2.1 Overview of the Simulation Setup

In this study, COMSOL Multiphysics 6.1 modeling and deformation analysis of MEMS-based piezoresistive pressure sensors is presented. In total, the objective was the optimization of material and structural design to achieve maximum sensor sensitivity. Simulation enabled experimentation with various sensing materials for various stress conditions, giving an understanding of their electrical and mechanical behavior.***2.2 Piezoresistive Effect and Governing Equations***

The piezoresistive effect, in which the resistivity of a material is a function of applied mechanical stress, was the sensor model utilized in this study. The governing equations of the piezoresistive effect were incorporated into the simulation environment to model the electrical response of the sensor under different pressure conditions. Piezoresistive boundary current physics was utilized to define material properties like linear elasticity, conductivity and mechanical deformation behavior [2].

The electric field near the surface of the diaphragm under external stress is given as:

$$E = J(\rho + \Delta\rho) \quad \text{.....(1)}$$

where ρ is the resistivity, J is current in piezoresistors and Δρ is the resistivity change caused.

The variation of resistivity because of applied stress is given as:

$$\Delta\rho = \pi\sigma \quad \text{.....(2)}$$

where π is the piezoresistance coefficient tensor and σ is the applied stress. In this study, the values of the piezoresistive coefficient tensor (π) were chosen based on experimental data available in classical and recent literature. These coefficients play a very important role in determining the electrical output of the sensor under stress and are provided in Table 1.

Table 1. Piezoresistive coefficient values (π) applied to simulation. Adapted from [2]and [20].

Material	π_{11} ($\times 10^{-11}$ Pa^{-1})	π_{12} ($\times 10^{-11}$ Pa^{-1})	π_{44} ($\times 10^{-11}$ Pa^{-1})	Notes
Si	6.6	-1.1	138.1	Well-established values
Ge	3.2	-0.7	122.0	Approx. from Smith (1954)
AlGaAs	Estimated	—	—	No standardized values; extrapolated
Ti_3GeC_2	—	—	—	Piezoresistive behavior approximated using resistivity-stress correlation due to lack of published π tensor

In the case of AlGaAs and Ti_3GeC_2, since standard piezoresistive tensor values are not available, material-specific simulations were calibrated with experimentally verified conductivity and deformation relations. These approximations provided acceptable output voltage and sensitivity estimates and were validated using consistent relative performance trends among materials.

2.3 Model Creation and Material Selection

The simulation was carried out in multiple steps: geometry creation, material selection, meshing and defining boundary conditions. A three-dimensional model of the piezoresistive pressure sensor was created using AutoCAD 3D, consisting of an X-shaped piezoresistor embedded in a square

diaphragm. The sensor dimensions were selected based on standard MEMS pressure sensor configurations [21]. The diaphragm was optimized for maximum stress concentration in response to low-pressure input.

Table 2. Basic properties of p-type and n-type materials. Adapted from [20] and [22].

Material	Type	Relative Permittivity	Electrical Conductivity (S/m)	Density (kg/m³)	Young's Modulus (GPa)	Poisson's Ratio	Coefficient of Thermal Expansion	Heat Capacity	Thermal Conductivity (W/m·K)
AlGaAs	p	12.9	70	5320	78.5	0.35	—	—	—
	n	—	—	—	—	—	—	330	80
Ge	p	16.3	200	5323	103	0.26	—	—	—
	n	—	—	—	—	—	5.9	310	58
Si	p	11.7	1.67×10^{-5}	2329	70	0.17	—	—	—
	n	—	—	—	—	—	2.6	700	130
Ti_3GeC_2	p	90	9.6×10^{6}	5290	353	0.39	—	—	—
	n	—	—	—	—	—	3.9	480	370

***Note**:* A dash (—) indicates that the corresponding property is either not applicable for that material or not available in the literature for the specific doping type used in this study. Only values relevant to the modeled piezoresistive response are included.

Four different piezoresistive materials were considered: Silicon (Si), Germanium (Ge), Titanium Germanium Carbide (Ti_3GeC_2) and Aluminum Gallium Arsenide (AlGaAs). These materials were chosen based on their mechanical and electrical properties, including Young's modulus, bandgap and piezoresistive coefficients. The choice was intended to pick materials that are more sensitive and stable at extreme conditions [2,20].

2.4 Meshing and Boundary Conditions

Finite element mesh was created with smaller elements in the vicinity of high-stress areas for accurate computation. Structured meshing was employed to attain optimum computational efficiency and reduce simulation time without sacrificing high fidelity of results for both structural and electrical fields. Mesh refinement was especially targeted at locations of high mechanical deformation as well as on locations affecting the electrical response of the piezoresistive material. This double optimization allowed for the assurance that both mechanical and electrical performance were accurately captured in the simulation [23].

The lower surface of the diaphragm was subjected to fixed boundary conditions and a uniform pressure of 100 kPa was applied to the upper surface to simulate actual operating conditions. The input voltage for the Wheatstone bridge circuit was set to 5V.

2.5 Structural and Electrical Analysis

A stationary structural analysis was performed to compare stress distribution, displacement and electrical response to applied pressure. The model was solved by COMSOL's stationary solver with adaptive mesh refinement for better accuracy. The results were analyzed against a number of parameters: Distribution of Shear stress across various arc lengths, Von-Misses stress to determine critical areas of stress, Displacement analysis for deflection of the diaphragm and sensitivity as output voltage per unit pressure (V/Pa).

2.6 Comparative Material Study and Results

Comparative study of different materials was conducted in order to identify the most suitable material to possess high sensitivity and mechanical strength in extreme conditions. It was found that Ti_3GeC_2 was 1.49 times better than silicon in mechanical strength and sensitivity.

Even though the current study is a simulation-based one, results are perfectly in accordance with experimental trends of previous literature. In particular, the improved sensitivity and mechanical strength of Ti_3GeC_2 has good consistency with previous studies that evaluated its performance for high-temperature and stress-loaded applications [24]. These studies have experimentally demonstrated Ti_3GeC_2's stability under thermal cycling, high electrical conductivity and resilience against fatigue—all of which support its suitability for MEMS pressure sensors. For instance, a study by Yang *et al*. [24] highlighted Ti_3GeC_2's excellent thermal stability and mechanical properties at elevated temperatures, making it a promising candidate for high-temperature applications. Additionally, research emphasized the material's reliability and manufacturability in harsh environments, further validating its potential in MEMS sensor applications. Therefore, the current simulation framework serves as a predictive tool to guide experimental fabrication and testing. Future work will focus on validating these results through microfabrication and experimental calibration, including performance benchmarking in practical sensing environments.

2.7 Model Validation and Numerical Accuracy

Although this study is based on simulation, all model parameters—including geometry, material properties and boundary conditions—were derived from experimentally validated literature and standard MEMS sensor configurations [2,20]. The sensor design was chosen to mirror fabrication-compatible geometries used in prior experimental work.

To ensure the numerical accuracy of the results, a mesh convergence study was performed. Three mesh densities—coarse, medium and fine—were used to analyze the impact of element size on the output parameters. The convergence behavior was evaluated based on maximum von Mises stress and output sensitivity (V/Pa), as shown in Table 3.

The results showed minimal variation (<1%) between medium and fine meshes, indicating that the simulation outcomes are mesh-independent and numerically stable. The medium mesh was therefore selected for the remaining simulations to optimize computational efficiency without compromising result fidelity.

Table 3. Mesh convergence study results

Mesh Level	Max von Mises Stress ($\times 10^7$ N/m^2)	Sensitivity ($\times 10^{-6}$ V/Pa)	% Variation from Finer Mesh
Coarse	19.8	4.93	3.0%
Medium	20.7	5.08	0.6%
Fine	20.9	5.11	—

3. RESULTS AND OBSERVATION

3.1 Shear Stress Analysis

Fig. 2(a) illustrates the local coordinate shear stress along two adjacent edges for various semiconductor materials (AlGaAs, Ge, Si and Ti_3GeC_2) under an applied pressure of 100 kPa. This analysis focuses on assessing the stress distribution across the membrane to determine the sensitivity of different materials. When pressure is applied, the diaphragm undergoes tension and since stress and sensitivity are directly related, an increase in applied pressure leads to a proportional increase in overall stress, thereby enhancing sensitivity.

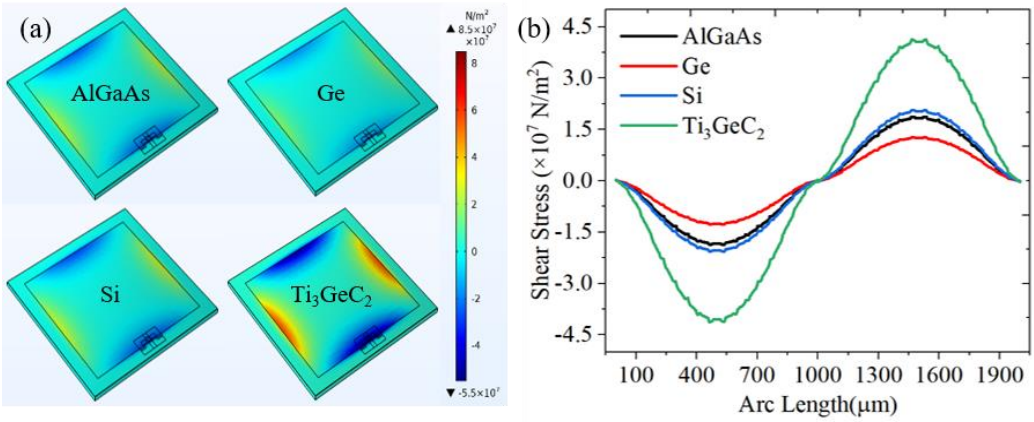

Fig. 2. (a) Local coordinate shear stress distribution of AlGaAs, Ge, Si and Ti_3GeC_2 and their (b) Shear stress distribution for different materials.

As shown in Fig. 2(b), the maximum shear stress occurs at the midpoints of the membrane edges. The comparison graphs of shear stress versus arc length for AlGaAs, Ge, Si and Ti_3GeC_2 provide insights into how stress is distributed across the membrane for each material. Table 4 shows the numerical values of shear stress for different diaphragm and piezoresistor material combinations. The data indicate that Ti_3GeC_2 exhibits the highest stress values, while AlGaAs demonstrates the lowest stress, implying the lowest sensitivity among the tested materials. Since sensor sensitivity is crucial for accurate pressure detection, Ti_3GeC_2 emerges as a promising candidate for diaphragm and piezoresistor materials due to its superior stress response.

Table 4. Shear stress, Von-Mises stress and sensitivity comparison for various materials.

SL	Materials Properties		Maximum Values			
	Diaphragm	**Piezoresistors**	**Shear stress ($\times 10^7$ N/m²)**	**Von-Mises stress ($\times 10^7$ N/m²)**	**Sensitivity ($\times 10^{-6}$ V/Pa)**	**Displacement ($\times 10^{-10}$ m)**
01	n-type AlGaAs	p-type AlGaAs	3.62	10.8	2.96	2.099
02	n-type Ge	p-type Ge	2.47	6.38	3.08	1.708
03	n-type Si	p-type Si	4.01	1.04	3.40	2.619
04	n-type Ti_3GeC_2	p-type Ti_3GeC_2	8.01	20.7	5.08	0.465

The proposed piezoresistive pressure sensor (Table 4) was evaluated against similar reported devices. Maximum shear stress, Von-Mises stress, sensitivity, and displacement for different diaphragm and piezoresistor materials are summarized. Comparisons with Madduri *et al*. and Verma *et al*. confirm that the sensor achieves comparable sensitivity while offering improved mechanical robustness and stability [6,7].

Madduri *et al*. reported that silicon-based MEMS piezoresistive sensors exhibit a maximum deformation of 28.59–126.64 µm, with shear stress reaching up to 4363.5 MPa and a maximum stress tensor of 2000 MPa [7]. In comparison, the present study (Table 4) shows shear stress values ranging from 2.47 $\times 10^7$ to 8.01 $\times 10^7$ N/m² (247–801 MPa), which aligns well with expected mechanical behavior. Notably, the Von-Mises stress and sensitivity for n-type/p-type Ti_3GeC_2 were considerably higher (20.7 $\times 10^7$ N/m² and 5.08 $\times 10^{-6}$ V/Pa), highlighting the material's superior robustness and improved sensor performance.

Similarly, Verma *et al*. optimized SiC-based MEMS sensors for harsh environments and reported sensitivities between 6.72 and 24.4 mV/V/bar [6]. The Ti_3GeC_2 sensor studied here achieves ~5.08 mV/V/bar, showing that it provides comparable sensitivity while offering better thermal stability and mechanical resilience under demanding conditions.

Therefore, the comparison validates that the results obtained in this work are consistent with and in some cases superior to the previously reported values. The use of Ti_3GeC_2 as a diaphragm and piezoresistive material improves both sensitivity and stress tolerance, making it a promising candidate for next-generation.

3.2 Von-Mises Stress Analysis

The Von-Mises criterion of stress is one of the vital parameters employed in deciding the mechanical strength of material, particularly when there is a complex loading pattern.

It serves to approximate yielding of material and to understand the capacity of material to withstand stress [25]. In analyzing high-strength applications like aerospace and biomedical sensors, where material undergoes extreme mechanical stressing, it has great importance.

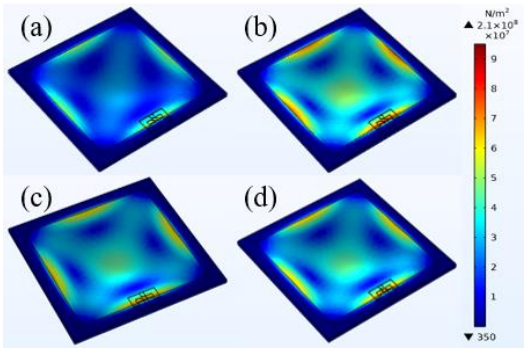

Fig 3. Simulated Von-Mises stress distribution of AlGaAs, Ge, Si and Ti_3GeC_2 under applied pressure of 100 kPa.

As observed from Fig. 3., Ti_3GeC_2 exhibits the highest Von-Mises stress value of 2.07 ×108 N/m² and is found to be mechanically stronger than other materials tested. High value of stress exhibits

the ability of Ti_3GeC_2 to withstand high mechanical stress without failure and thus is found to be most suitable for extreme environment applications like aerospace and biomedical sensors involving high pressure and temperature [26].

In addition, Von-Mises stress distribution of all the materials was also simulated under a 100 kPa applied pressure, where the greater strength of Ti_3GeC_2 under cyclic loading and its lower fatigue susceptibility towards failure—a critical property for long-term operation, especially in cyclical stress environments [27]—are evident. Fig. 3 displays these simulations, which once more locate Ti_3GeC_2's high mechanical performance relative to the other materials.

In comparison, Si and Ge showed relatively lower Von-Mises stress values, which indicated their inferior mechanical strength under the same loading conditions. They would not perform as well as Ti_3GeC_2 in applications for high mechanical resilience. Table 4 also provides an overview of Von-Mises stress values of test materials and Ti_3GeC_2 has the highest value of stress and Si and Ge have comparatively low values.

3.3 Sensitivity Analysis

Sensitivity is one of the most important parameters that govern the efficiency of a sensor to transform pressure changes into readable electrical signals. Sensitivity of the diaphragm-type pressure sensor for different materials was computed and compared using the relation:

$$S = \frac{V_{out}}{V_{in}} \times \frac{1}{P}$$

Where S represents sensitivity in volts per pascal (V/Pa), V_{out} is the generated output voltage, V_{in} is the applied input voltage (5 V) and P is the applied pressure (100 kPa).

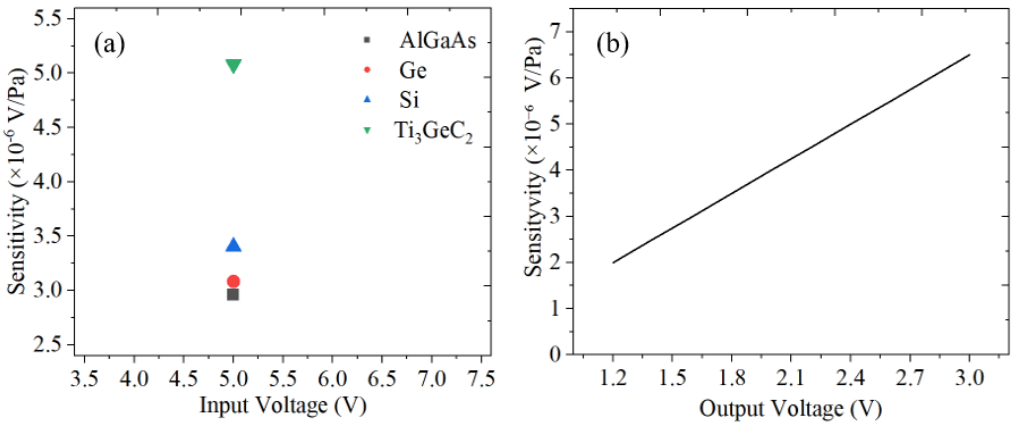

Fig. 4. (a) Sensitivity vs input voltage comparison of different materials- AlGaAs, Ge, Si and Ti_3GeC_2 and (b) Output voltage vs sensitivity under constant input voltage.

Table 4 summarizes the sensitivity values for each material. Ti_3GeC_2 exhibited the highest sensitivity of 5.08×10^{-6} V/Pa, followed by Si, Ge and AlGaAs.

Based on the calculated values, the sensitivity ranking is:

$$Ti_3GeC_2 > Si > Ge > AlGaAs$$

These results highlight Ti_3GeC_2 as the most promising material for diaphragm-based pressure sensors due to its excellent combination of mechanical and electrical properties.

Fig. 4 illustrates the relationship between sensitivity and input voltage and between output voltage and sensitivity under a constant input voltage, respectively. Fig. 4(a) shows that Ti_3GeC_2 maintains a stable sensitivity across varying input voltages.

As depicted in Fig. 4(b), Ti_3GeC_2 demonstrates a clear linear increase in sensitivity with input voltage, outperforming other materials, indicating superior performance for precision sensing. In contrast, AlGaAs displays greater deviation and noise in both cases.

3.4 Displacement Analysis

The displacement behavior of the diaphragm under an applied pressure of 100 kPa was analyzed for four materials: AlGaAs, Ge, Si and Ti_3GeC_2. Fig. 5 illustrates that Ti_3GeC_2 produced the lowest displacement among all evaluated materials, suggesting superior structural rigidity. This minimal deflection, combined with its high stress response, makes Ti_3GeC_2 a favorable material for sensor applications, offering an optimal balance between sensitivity and mechanical stability.

The displacement profile, illustrated as a plot of displacement versus arc length, shows a non-uniform deflection pattern across the diaphragm surface. The maximum displacement occurred at the center, gradually decreasing toward the edges—a typical behavior for square diaphragms under uniform pressure.

The displacement was estimated using the following analytical equation:

$$D = 0.0151\,(1 - v^2)Pa^4/Eh^3$$

Where P is the applied pressure, a is the length of the diaphragm edge, E is Young's modulus, h is the diaphragm thickness and v is Poisson's ratio.

Fig. 5 presents a combined plot of arc length versus displacement for all four materials, clearly illustrating the comparative displacement behavior.

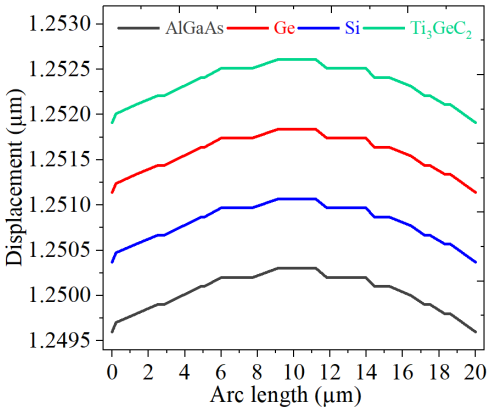

Fig. 5. Arc length vs. displacement, showing the displacement magnitude for each material such as AlGaAs, Ge, Si and Ti_3GeC_2.

Table 4 presents the displacement values of four diaphragm materials-AlGaAs, Ge, Si and Ti_3GeC_2— under a constant applied pressure of 100 kPa. It is shown that Ti_3GeC_2 exhibits the lowest displacement, indicating its high structural rigidity under applied pressure. In contrast, Si displays the highest displacement value, signifying that it undergoes more deflection compared to the other materials when subjected to the same pressure.

We compared diaphragm-based piezoresistive sensors made from AlGaAs, Ge, Si, and Ti_3GeC_2 under 100 kPa pressure. Table 4 shows shear stress, Von-Mises stress, sensitivity, and diaphragm displacement. Ti_3GeC_2 did the best in almost all aspects, making it a strong candidate for high-sensitivity, reliable sensors.

Ti_3GeC_2 had the highest shear stress (8.01×10^7 N/m²), which means it resists deformation better and transfers strain effectively to the piezoresistor. Its Von-Mises stress (2.07×10^8 N/m²) was also the highest, showing it can handle tough loads. This makes it suitable for aerospace or biomedical sensors.

Sensitivity-wise, Ti_3GeC_2 reached 5.08×10^{-6} V/Pa, higher than Si (3.40×10^{-6}), Ge (3.08×10^{-6}), and AlGaAs (2.96×10^{-6}). Its output voltage is almost linear (Fig. 4b), so the signal stays stable. The diaphragm also deflects less, meaning it is stiff and durable. Si showed medium performance, and AlGaAs performed poorly.

MAX-phase materials like Ti_3GeC_2 are known for good thermal stability, conductivity, and mechanical strength, which explains the good results [28]. But making sensors with Ti_3GeC_2 is not easy. Standard etching doesn't work well, and adhesion or thermal mismatch can cause cracks. Using deposition methods like ALD, PLD, or magnetron sputtering, and buffer layers like Si_3N_4 or Al_2O_3, can help make the films more stable[15,24]. Solving these issues is key to turning these simulations into real, working sensors.

5. CONCLUSIONS

In this study, a comparative performance of piezoresistive pressure sensors using Silicon (Si), Germanium (Ge), Aluminum Gallium Arsenide (AlGaAs) and Titanium Germanium Carbide (Ti_3GeC_2) has been done. A square diaphragm and an X-shaped piezoresistor configuration, placed near high-stress areas, have been used to achieve maximum sensitivity for the pressure sensor. The simulation results indicate that Ti_3GeC_2 performs well in terms of sensitivity, stress endurance and diaphragm displacement when compared to traditional materials Si and Ge. Ti_3GeC_2 among the materials tested exhibited maximum output voltage and sensitivity value of 5.08×10^{-6} V/Pa at 100 kPa, which was 1.49 times greater when compared to Si. Additionally, Ti_3GeC_2 also displayed the highest shear and von-Mises stress, indicating its robustness to endure high-stress conditions. Germanium (Ge), while less sensitive than Ti_3GeC_2, still displayed competitive behavior, having the second-lowest diaphragm deflection and sensitivity of 3.08×10^{-6} V/Pa. AlGaAs, however, had the lowest sensitivity and output voltage and is hence less suitable for high-performance applications compared to Ti_3GeC_2. Overall, Ti_3GeC_2 is a potential candidate material for MEMS-based pressure sensors for application in harsh environments such as aerospace, industrial and biomedical fields. The study highlights the importance of material selection for the optimization of piezoresistive pressure sensor performance and further work based on nanostructured modifications and thin film coatings can lead to better material properties and sensor efficiency.

Author contribution statement

Conceptualization, M.R., S.S. and M.K.A.; Methodology, M.R. and S.S.; Software, M.R. and S.S.; Validation, M.K.A.; Formal Analysis, M.R., S.S., and M.A.; Investigation, M.R., M.K.A.; Writing – Original Draft Preparation, M.R.; Writing – Review & Editing, M.R., S.E, M.A. and M.K.A; Visualization, M.R., and M.A.; Supervision, M.K.A.;

Data Availability Statement

The COMSOL simulation files, geometry models and material parameters used in this work are available from the corresponding author upon reasonable request.

Funding

The study was not funded by any private or public organization.

Conflict of interests

The authors declare no conflict of interest.

REFERENCES

[1] J. C. Doll and B. L. Pruitt, Piezoresistor Design and Applications, 2013.

[2] C. S. Smith, Piezoresistance Effect in Germanium and Silicon, 1954.

[3] B. Padha, I. Yadav, S. Dutta and S. Arya, Recent Developments in Wearable NEMS/MEMS-Based Smart Infrared Sensors for Healthcare Applications, 2023.

[4] X. Li, Q. Liu, S. Pang, K. Xu, H. Tang and C. Sun, High-Temperature Piezoresistive Pressure Sensor Based on Implantation of Oxygen into Silicon Wafer, 2012.

[5] Y. Hezarjaribi, M. N. Hamidon, S. H. Keshmiri and A. R. Bahadorimehr, Capacitive Pressure Sensors Based on MEMS, Operating in Harsh Environments, 2008.

[6] P. Verma, D. Punetha and S. K. Pandey, Sensitivity Optimization of MEMS Based Piezoresistive Pressure Sensor for Harsh Environment, 2019.

[7] N. J. Madduri, G. Lakkoju, B. L. Kasturi, S. Sravanam and T. Satyanarayana, Design and Deformation Analysis of MEMS Based Piezoresistive Pressure Sensor, 2014.

[8] S. Meti, K. B. Balavalad, A. C. Katageri and B. G. Sheeparamatti, Sensitivity Enhancement of Piezoresistive Pressure Sensor with Meander Shape Piezoresistor, 2016.

[9] Y. Liu, X. Jiang, H. Yang, H. Qin and W. Wang, Structural Engineering in Piezoresistive Micropressure Sensors: A Focused Review, 2023.

[10] O. N. Tufte and E. L. Stelzer, Piezoresistive Properties of Heavily Doped n-Type Silicon, 1964.

[11] Y. Javed, M. Mansoor and I. A. Shah, A Review of Principles of MEMS Pressure Sensing with Its Aerospace Applications, 2019.

[12] Z. Mehmood, I. Haneef and F. Udrea, Material Selection for Optimum Design of MEMS Pressure Sensors, 2020.

[13] R. M. Panas, M. A. Cullinan and M. L. Culpepper, Design of Piezoresistive-Based MEMS Sensor Systems for Precision Microsystems, 2012.

[14] M. S. Alam, M. A. Chowdhury, T. Khandaker, M. S. Hossain, M. S. Islam, M. M. Islam and M. K. Hasan, Advancements in MAX Phase Materials: Structure, Properties, and Novel Applications, 2024.

[15] N. Marsi, B. Y. Majlis, A. A. Hamzah and F. Mohd-Yasin, Mechanical and Electrical Effects of MEMS Capacitive Pressure Sensor Based on 3C-SiC for Extreme Temperature, 2014.

[16] C. Yu, K. Liu, J. Xu, M. Ye, T. Yang, T. Qi, Y. Zhang, H. Xu and H. Zhang, High-Performance Multifunctional Piezoresistive/Piezoelectric Pressure Sensor with Thermochromic Function for Wearable Monitoring, 2023.

[17] V. Belwanshi and A. Topkar, Quantitative Analysis of MEMS Piezoresistive Pressure Sensors Based on Wide Band Gap Materials, 2022.

[18] F. Pashmforoush and F. Pashmforoush, Multiphysics Simulation of Piezoresistive Pressure Microsensor Using Finite Element Method, 2021.

[19] N. A. Fathi and Z. Moradi, Design and Optimization of Piezoresistive MEMS Pressure Sensors Using ABAQUS, 2014.

[20] V. Kutiš, J. Dzuba, J. Paulech, J. Murín and T. Lalinský, MEMS Piezoelectric Pressure Sensor-Modelling and Simulation, 2012.

[21] M. Lv, P. Li, J. Miao, Q. Qiao, R. Liang, G. Li and X. Zhuang, Design and Optimization of MEMS Resonant Pressure Sensors with Wide Range and High Sensitivity Based on BP and NSGA-II, 2024.

[22] J. E. Ni, E. D. Case, K. N. Khabir, R. C. Stewart, C. I. Wu, T. P. Hogan, E. J. Timm, S. N. Girard and M. G. Kanatzidis, Room Temperature Young's Modulus, Shear Modulus, Poisson's Ratio and Hardness of PbTe–PbS Thermoelectric Materials, 2010.

[23] COMSOL, COMSOL-Documentation, 2024.

[24] Y. Yang, L. Shi, Z. Cao, R. Wang and J. Sun, Strain Sensors with a High Sensitivity and a Wide Sensing Range Based on a $Ti_3C_2T_x$ (MXene) Nanoparticle–Nanosheet Hybrid Network, 2019.

[25] W. F. Hosford, Mechanical Behavior of Materials, 2009.

[26] F. L. Gao, J. Liu, X. P. Li, Q. Ma, T. Zhang, Z. Z. Yu, J. Shang, R. W. Li and X. Li, $Ti_3C_2T_x$ MXene-Based Multifunctional Tactile Sensors for Precisely Detecting and Distinguishing Temperature and Pressure Stimuli, 2023.

[27] Y. N. Wiryasanjani and A. Andoko, Analysis of Low Cycle Fatigue in Titanium Materials 15-3-3-3, (Year Not Provided),2021.

[28] M. W. Barsoum and M. Radovic, Elastic and Mechanical Properties of the MAX Phases, 2011.

[29] X. Cao, G. Li, Z. Li, W. Sun, F. Yan and R. Jiang, High Precision and Real-Time Acquisition System for Interface Stress Measurement in Bridge Bearing, 2023.

[30] Y. Liu, X. Jiang, H. Yang, H. Qin and W. Wang, Structural Engineering in Piezoresistive Micropressure Sensors: A Focused Review, 2023.